Ring opening of aromatic heterocycles by uranium complexes

Selma Duhović, Marisa J. Monreal, Paula L. Diaconescu*

Department of Chemistry & Biochemistry, University of California, Los Angeles, CA 90095, USA

ABSTRACT

The reactivity of a uranium dibenzyl complex supported by a ferrocene-diamide ligand toward aromatic N-heterocycles was investigated. Although ring opening occurred, a complicated behavior was observed with 1-methylbenzimidazole and benzoxazole. On the other hand, when a uranium benzyl η^2-N,C-benzimidazole complex reacted with quinoline, alkyl transfer to the pyridine ring was observed.

© 2010 Elsevier B.V. All rights reserved.

1. Introduction

Examples of homogeneous, early transition metal-mediated C–N bond cleavage in aromatic N-heterocycles have been limited to tantalum [1–7], niobium [8–11], and titanium [12,13], and employ reactive metal entities [14]. In the tantalum and niobium cases, the formation of metal–nitrogen multiple bonds is proposed to drive these reactions. In the case of titanium, a titanium alkylidyne is a proposed intermediate. Recently, a few examples of aromatic N-heterocycle cleavage by late transition metal complexes have also been reported; these systems involve rhenium [15,16] and tungsten metal centers [17].

Thorium complexes that ring-opened pyridine N-oxide [18] and uranium complexes that cleaved pyrazole [19] are also known. Our group has been investigating the reactivity of group 3 metal [20–24] and uranium alkyls [25,26] supported by a 1,1′-ferrocenylene-diamide ligand [27–29] toward aromatic N-heterocycles [22,30–35]. We have shown that imidazole ring opening can take place with these electrophilic metal centers. In particular, the reactivity of a uranium dibenzyl complex has held our attention since $(NN^{fc})U(CH_2Ph)_2$, **1-(CH_2Ph)_2** (NN^{fc} = fc(NSi^{t}BuMe$_2$)$_2$, fc = 1,1′-ferrocenylene) [26], has two alkyl groups that can both engage in reactions with the same substrate. For example, we reported a novel C–H activation by **1-(CH_2Ph)_2**, showing that both benzyl ligands reacted with an sp^2-C–H bond of 1-methylimidazole (mi) to give **2^{mi}-mi** (Scheme 1) [31,36]. We also showed that, in addition to the double C–H activation, an interesting cascade of functionalization reactions could be thermally induced. Specifically,

upon heating, one of the η^2-N,C-imidazolyl and the coordinated imidazole ligands in **2^{mi}-mi** underwent C–C coupling to give **3^{mi}**, a process followed by the ring opening of the dearomatized ring and the migratory insertion of the remaining imidazolyl ligand, ultimately leading to an isomeric mixture of **4A** and **4B** (Scheme 1) [31]. Herein, we report the reactions of **1-(CH_2Ph)_2** with other aromatic heterocycles; substrates analogous to imidazole, such as benzoxazole and benzothiazole, as well as quinoline were studied.

2. Results and discussion

The mechanistic proposal shown in Scheme 1 was supported by the analogous reactions of a pyridyl–benzyl complex with benzoxazole and benzothiazole [30] and by the characterization of a C–C coupled product based on 1-methylbenzimidazole [31,36]. This complex, **3^{mbi}**, is analogous to **3^{mi}** (shown in Scheme 1). At the time when the cascade of reactions involving 1-methylimidazole was reported, an analogous transformation for 1-methylbenzimidazole was not obvious. Later, we reported that the C–C coupling reaction leading to **3^{mbi}** is a reversible transformation [36].
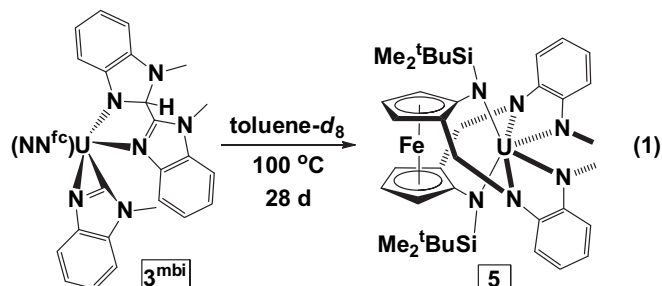

* Corresponding author.
    E-mail address: pld@chem.ucla.edu (P.L. Diaconescu).
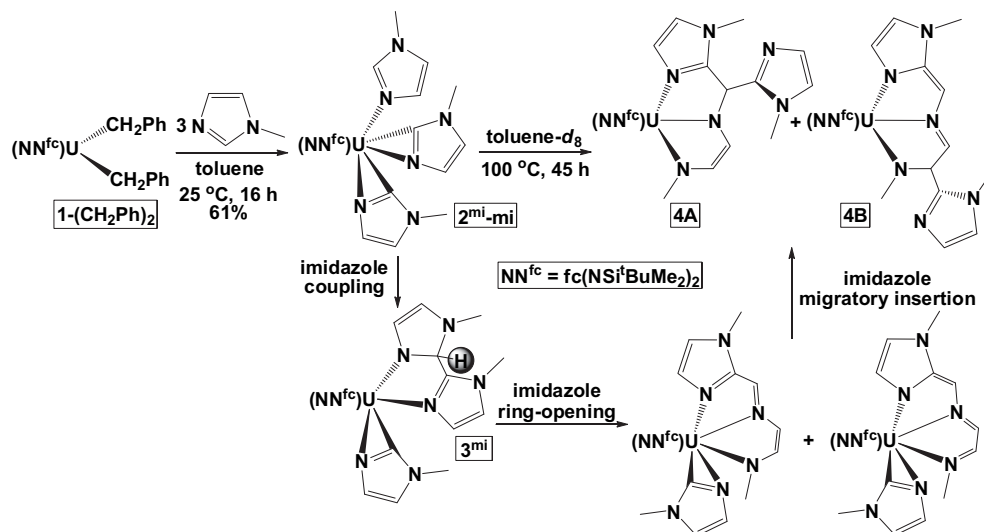
Scheme 1. Reactions of 1-methylimidazole mediated by **1-(CH$_2$Ph)$_2$**.

Repeating the reaction of **1-(CH$_2$Ph)$_2$** with three equivalents of 1-methylbenzimidazole, followed by prolonged heating, led invariably to complicated reaction mixtures [31]. In one instance, one of the products, **5** (Eq (1)), was isolated by fractional recrystallization and characterized by X-ray crystallography (Fig. 1). A rational synthesis of **5**, directly from **2^{mbi}**, which contains only two benzimidazole fragments, was attempted, but heating a toluene-d_8 solution of **2^{mbi}** led to a reaction mixture similar to the one obtained from **3^{mbi}**.

It is important to note that although **5** was separated by fractional crystallization and isolated, it is not the major product of the thermal decomposition of **2^{mbi}** or **3^{mbi}**. Although a complicated ring-opening and protonation/deprotonation mechanism must operate in order for **5** to form, such a sequence of reactions indicates that the cleavage of the imidazole ring may not be conditioned by its dearomatization as a result of coupling with another hetero aromatic ring. However, given the complexity of the reactions that led to **5**, it is difficult to make definitive assertions in that respect.
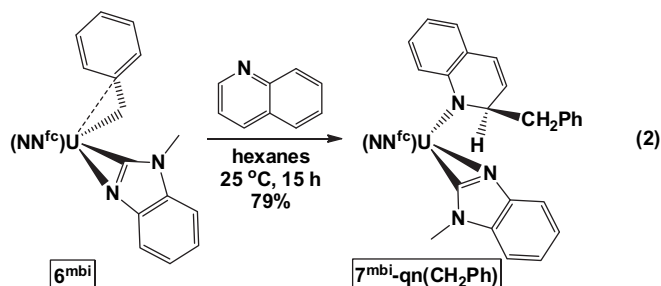
The sequential C–H activation of two equivalents of 1-methylbenzimidazole was also possible and the product of only one event, the uranium benzyl complex **6^{mbi}**, was isolated [36]. The reaction of **6^{mbi}** with quinoline was investigated in order to determine whether this substrate undergoes C–H activation, as observed with a scandium benzyl supported by the same ferrocene-diamide ligand [22], or alkyl transfer, as observed with isoquinoline and group 3 metal benzyl complexes [23]. Consequently, when **6^{mbi}** was mixed with quinoline in hexanes, at room temperature, no toluene formation was observed after 15 h, ruling our C–H activation (Eq (2)).

The isolation and characterization of the major product, **7^{mbi}-qn** (**CH$_2$Ph**), by X-ray crystallography indicated that alkyl transfer

occurred from uranium to the 2-position of quinoline (Fig. 2). Metrical parameters are consistent with the dearomatization of the pyridine ring. For example, the C–C distances are 1.412(14), 1.447 (18), 1.333(17), and 1.487(14) Å, with the longest distance to the sp^3-carbon atom. Also, the U–N distance to the dearomatized pyridine ring, 2.3034(64) Å, is only 0.08 Å longer than the U–N distances to the ferrocene-diamide ligand (2.2196(66) and 2.2342 (69) Å). The NCC angles of 113.01(92) and 111.05(73)° and the CCC angle of 110.77(76)° around the sp^3-carbon atom are in agreement with this structural assignment. The dearomatized quinoline coordinates in an approximate κ^3-NCC fashion, as evidenced by the U–C21 and U–C29 distances of 2.9594(88) and 3.0432(91) Å, respectively, which are similar to the distances between uranium and the *ipso*-carbon atoms of the ferrocene diamide (2.8810(78) and 2.8896(80) Å). The solid-state structure also confirms the
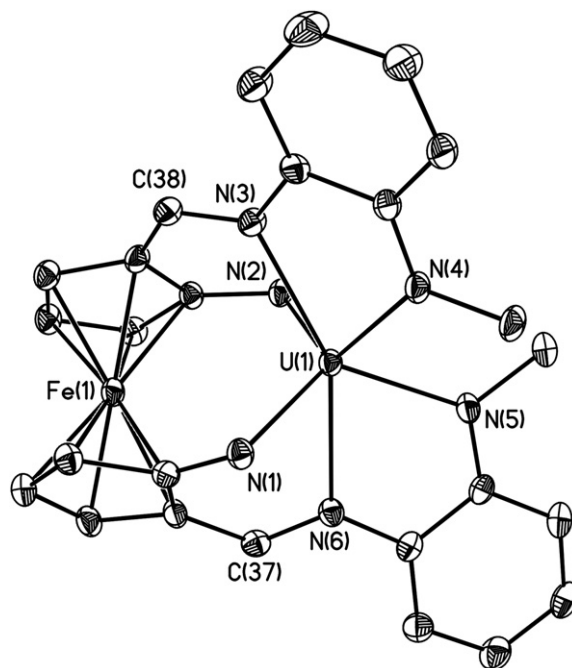

Fig. 1. Thermal-ellipsoid (50% probability) representation of 5. Hydrogen atoms and silyl groups were removed for clarity.
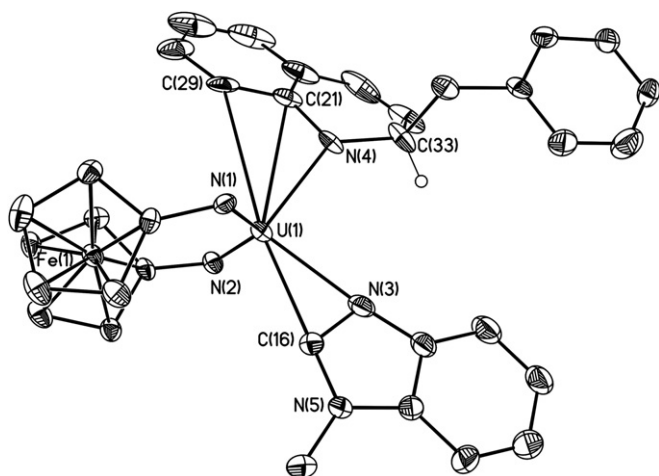
Fig. 2. Thermal-ellipsoid (35% probability) representation of 7^{mbi}-$qn(CH_2Ph)$. Irrelevant hydrogen atoms and silyl groups were removed for clarity.
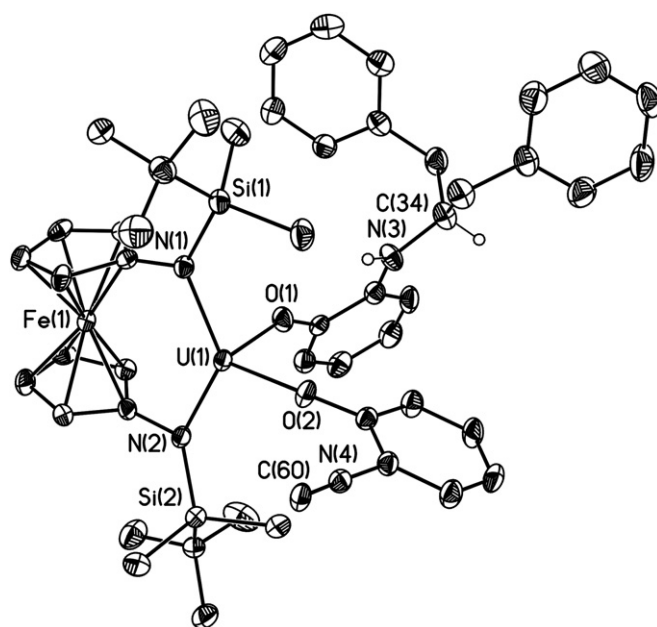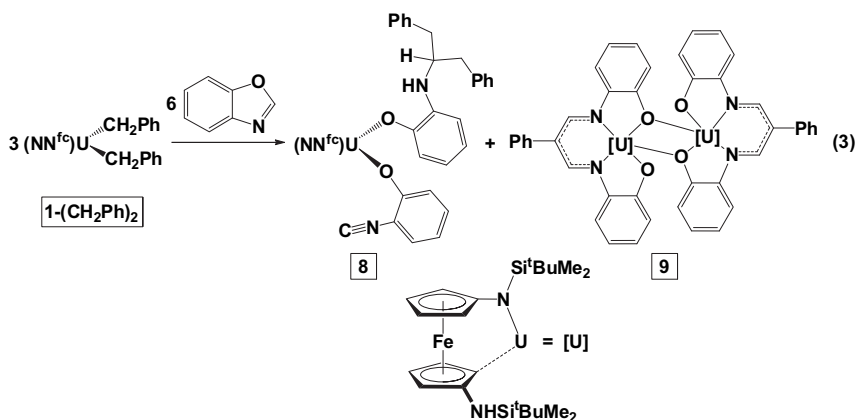

Fig. 3. Thermal-ellipsoid (50% probability) representation of 8. Irrelevant hydrogen atoms and silyl groups were removed for clarity.

presence of the imidazolyl ligand, which retained its η^2-N,C-coordination: the U–N_{mbi} distance of 2.4135(82) Å and the U–C_{mbi} distance of 2.4295(86) Å are similar to the analogous distances of 2.3708(24) and 2.4811(27) Å, respectively, in 6^{mbi} [36].

The reaction between **1-(CH₂Ph)₂** and two equivalents of benzoxazole was carried out to determine whether a behavior similar to that of benzimidazole would be observed. Although the conditions were modified numerous times in an attempt to favor the formation of a single product, all reactions consistently led to mixtures that proved difficult to separate and reproduce. The structures of two products **8** and **9** (Eq (3)), containing ring-opened oxazoles, were determined by single crystal X-ray diffraction (Figs. 3 and 4). Unfortunately, these products were difficult to purify for full characterization.

In order to explain the formation of **8**, we propose (Scheme 2) that benzyl transfer to a coordinated benzoxazole effects its ring opening and the formation of an imine group (**8-boz(CH₂Ph)**); this intermediate is susceptible to another benzyl migration to give **8-boz(CH₂Ph)₂**, which contains an amide functionality, likely coordinated to the uranium center. The polarization of the newly formed U–N bond may lead to the deprotonation of another benzoxazole molecule, also likely coordinated to the uranium center. The deprotonation of oxazoles, known to induce ring opening and formation of isonitriles [37,38], provides support for the above scenario leading to **8**. The formation of **9** seems even more complicated, but it must involve a C–H activation step since one of the benzyl groups is not part of the product. Furthermore, even

though the ferrocene ligand is still chelating through a weak interaction between uranium and one of the cyclopentadienyl carbon atoms, one of the ferrocene amides was protonated and dissociated.

3. Conclusions

The reactions of uranium alkyl complexes with aromatic N-heterocycles are substrate dependent. When benzoheterocycles containing two heteroatoms were employed, the reactions led to complicated mixtures. The products isolated from those mixtures indicated that cleavage of the heteroaromatic ring occurred in all cases. In order to arrive at those products, we proposed that, following ring opening, reactive intermediates were generated that engaged in subsequent transformations. It is interesting to note that the newly formed b-diketiminate in **9** is tetradentate and, because of its symmetry, could function as an ancillary ligand; however, its formation as part of a secondary product in the reaction of 1-(CH₂Ph)₂ with benzoxazole discouraged us from pursuing this idea. This complicated behavior observed with benzimidazole and benzoxazole was not repeated when a uranium benzyl η^2-N,C-benzimidazole complex reacted with quinoline, alkyl transfer to the pyridine ring being observed.
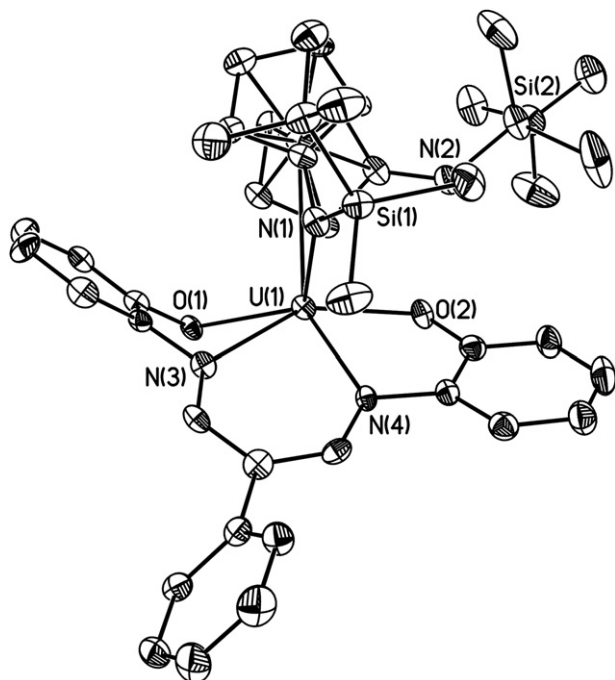
Fig. 4. Thermal-ellipsoid (50% probability) representation of **9**. Only the monomeric unit was represented (for a representation of the dimer, see Figure SX4a in the Supporting information); hydrogen and solvent atoms were removed for clarity.

4. Experimental

All experiments were performed under a dry nitrogen atmosphere using standard Schlenk techniques or an MBraun inert-gas glovebox. Solvents were purified using a two-column solid-state purification system by the method of Grubbs [39] and transferred to the glovebox without exposure to air. NMR solvents were obtained from Cambridge Isotope Laboratories, degassed, and stored over activated molecular sieves prior to use. Uranium turnings were purchased from Argonne National Laboratories.
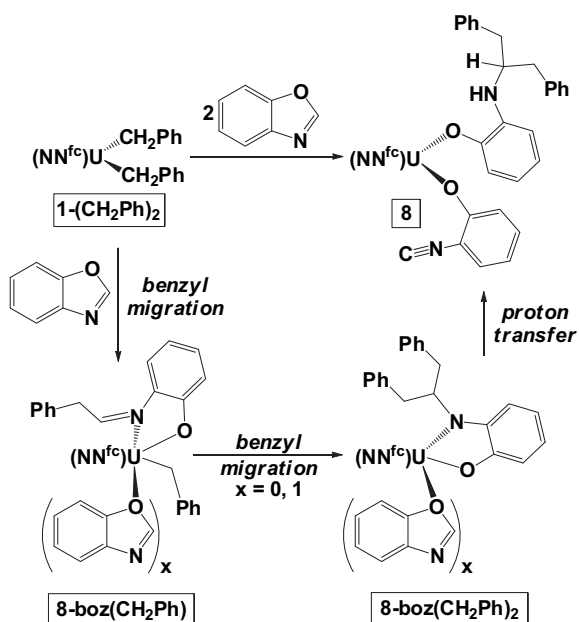
Scheme 2. Reaction of **1-(CH$_2$Ph)$_2$** with benzoxazole and proposed mechanism.

Compounds **1-(CH$_2$Ph)$_2$** [26] and **6^{mbi}** [36] were prepared following published procedures. The aromatic heterocycles were distilled or recrystallized before use; all other materials were used as received. ^{1}H NMR spectra were recorded on Bruker300 or Bruker500 spectrometers (supported by the NSF grant CHE-9974928) at room temperature in C$_6$D$_6$ unless otherwise specified. Chemical shifts are reported with respect to solvent residual peak, 7.16 ppm (C$_6$D$_6$). CHN analyses were performed by UC Berkeley Micro-Mass facility, 8 Lewis Hall, College of Chemistry, University of California, Berkeley, CA 94720.

4.1. Synthesis of **5**

A toluene solution of 1-methylbenzimidazole (0.0147 g, 1 equiv) was added to a toluene solution of **3^{mbi}** (0.1196 g) and allowed to stir vigorously at 100 °C for 28 d. The volatiles were removed under reduced pressure and the resulting dried, crude product was extracted with hexanes and filtered through Celite. Fractional crystallization from hexanes allowed single crystals of **5** to form and a ^{1}H NMR spectrum to be obtained. However, reproducing the initial reaction conditions did not allow the isolation of pure **5** for further characterization.

4.2. Synthesis of **7^{mbi}-qn(CH$_2$Ph)**

Quinoline (13.5 mg, 0.1 mmol) was dissolved in 2 mL of hexanes and slowly added to a stirring hexanes solution of **6^{mbi}** (89.9 mg, 0.1 mmol). The reaction mixture was stirred at room temperature for 15 h, filtered through Celite, and dried (crude yield: 79%, pure by ^{1}H NMR spectroscopy). The brown-yellow oil was redissolved in fresh hexanes, passed through Celite, and stored at −35 °C as a highly concentrated solution. Brown, block crystals suitable for X-ray structure analysis formed after 3 d. ^{1}H NMR (C$_6$D$_6$, 500 MHz, 25 °C), δ (ppm): 41.40, 41.13, 37.68, 34.37 (s, 3H each, SiCH$_3$), 27.12, 26.50 (s, 9H each, SiC(CH$_3$)$_3$), 2.20 (t, 2H, CH$_2$Ph), 1.86, −2.06, −16.99, −65.57 (t, 1H each, C$_5$H$_4$, aromatic-CH, or NC$_5$H$_3$), 4.17, 0.69, −4.08, −4.20, −5.19, −14.80, −23.62 (d, 1H each, C$_5$H$_4$, aromatic-CH, or NC$_5$H$_3$), −3.94, −3.98, −12.42, −14.16, −14.63, −14.70, −16.12, −19.03, −26.57, −32.52, −42.23, −82.59 (s, 1H each, C$_5$H$_4$, aromatic-CH, or NC$_5$H$_3$), −20.39 (s, 3H, NCCH$_3$). Anal. (%) Calcd. for C$_{46}$H$_{59}$FeN$_5$Si$_2$U (1032): C, 53.51; H, 5.78; N, 6.79. Found: C, 53.18; H, 5.43; N, 6.39.

4.3. Formation of **8** and **9**

A hexanes solution (10 mL) of **1-(CH$_2$Ph)$_2$** (94.7 mg, 0.11 mmol) was cooled to −78 °C for 30 min. Solid benzoxazole (14 mg, 0.11 mmol) that was kept at −35 °C was added and the reaction mixture was allowed to stir at room temperature overnight. The volatiles were removed under reduced pressure and an *n*-pentane solution of the resulting red solid was filtered through Celite. Yellow clusters of **8** and red blocks of **9** co-crystallized from a dilute diethyl ether solution. All attempts to separate and fully characterize the two products were not successful.

4.4. X-ray crystal structures

X-ray quality crystals were obtained from various concentrated solutions placed in a −35 °C freezer in the glovebox. Inside the glovebox, the crystals were coated with oil (STP Oil Treatment) on a microscope slide, which was brought outside the glovebox. The X-ray data collections were carried out on a Bruker AXS single crystal X-ray diffractometer using MoK$_\alpha$ radiation and a SMART APEX CCD detector. The data was reduced by SAINTPLUS and an empirical absorption correction was applied using the package SADABS. The structures were solved and refined using SHELXTL (Brucker 1998,

SMART, SAINT, XPREP AND SHELXTL, Brucker AXS Inc., Madison, Wisconsin, USA). All atoms were refined anisotropically and hydrogen atoms were placed in calculated positions unless specified otherwise. Tables with atomic coordinates and equivalent isotropic displacement parameters, with all the bond lengths and angles, and with anisotropic displacement parameters are listed in the cifs.

4.5. X-ray crystal structure of 5

X-ray quality crystals were obtained from a concentrated *n*-pentane solution. An *n*-pentane and half of a benzene solvent molecule were found in the unit cell. The solvent molecules were slightly disordered; this disorder was not modeled. A total of 47646 reflections ($-36 \leq h \leq 36$, $-25 \leq k \leq 25$, $-28 \leq l \leq 28$) was collected at $T = 100(2)$ K with $\theta_{max} = 30.74°$, of which 13970 were unique ($R_{int} = 0.0453$). The residual peak and hole electron density were 1.69 and -1.072 e A^{-3}. The least-squares refinement converged normally with residuals of $R_1 = 0.0327$ and GOF = 1.011. Crystal and refinement data for **5**: formula $C_{46}H_{65}N_6Si_2FeU$, space group $C2/c$, $a = 25.696(3)$, $b = 17.915(2)$, $c = 20.656(3)$, $\beta = 90.962$ $(1)°$, V = 9508(2) Å^3, Z = 8, $\mu = 3.795$ mm^{-1}, $F(000) = 4232$, $R_1 = 0.0536$ and $wR_2 = 0.0745$ (based on all 13970 data, $I > 2\sigma(I)$).

4.6. X-ray crystal structure of 7^{mbi}-qn(CH$_2$Ph)

X-ray quality crystals were obtained from a concentrated hexanes solution. A total of 81489 reflections ($-25 \leq h \leq 25$, $-26 \leq k \leq 25$, $-31 \leq l \leq 31$) was collected at $T = 100(2)$ K with $\theta_{max} = 28.33°$, of which 11284 were unique ($R_{int} = 0.1686$). The residual peak and hole electron density were 2.31 and -2.16 e A^{-3}. The least-squares refinement converged normally with residuals of $R_1 = 0.0628$ and GOF = 1.028. Crystal and refinement data for **7^{mbi}-qn(CH$_2$Ph)**: formula $C_{46}H_{59}N_5Si_2FeU$, space group $Pbca$, $a = 19.096$ (5), $b = 19.896(6)$, $c = 23.964(7)$, $\beta = 90°$, V = 9105(4) Å^3, Z = 8, $\mu = 3.961$ mm^{-1}, $F(000) = 4128$, $R_1 = 0.1363$ and $wR_2 = 0.1492$ (based on all 11284 data, $I > 2\sigma(I)$).

4.7. X-ray crystal structure of 8

X-ray quality crystals were obtained from a dilute diethyl ether solution. A toluene solvent molecule was found in the unit cell. A total of 25611 reflections ($-17 \leq h \leq 17$, $-19 \leq k \leq 18$, $-21 \leq l \leq 21$) was collected at $T = 100(2)$ K with $\theta_{max} = 29.15°$, of which 14015 were unique ($R_{int} = 0.0408$). The residual peak and hole electron density were 1.16 and -2.00 e A^{-3}. The least-squares refinement converged normally with residuals of $R_1 = 0.0409$ and GOF = 1.015. Crystal and refinement data for **8**: formula $C_{50}H_{61}N_4Si_2FeU$ C_7H_8, space group $P\bar{1}$, $a = 12.7226(14)$, $b = 14.0781(16)$, $c = 15.9396(18)$, $\alpha = 84.472(1)$, $\beta = 74.034(1)$, $\gamma = 80.301(1)°$, V = 2701.8(5) Å^3, Z = 2, $\mu = 3.350$ mm^{-1}, $F(000) = 1202$, $R_1 = 0.0613$ and $wR_2 = 0.0801$ (based on all 14015 data, $I > 2\sigma(I)$).

4.8. X-ray crystal structure of 9

X-ray quality crystals were obtained from a dilute diethyl ether solution. Four benzene solvent molecules were found in the unit cell. A total of 22640 reflections ($-14 \leq h \leq 14$, $-20 \leq k \leq 20$, $-22 \leq l \leq 22$) was collected at $T = 100(2)$ K with $\theta_{max} = 28.16°$, of which 12176 were unique ($R_{int} = 0.0562$). The residual peak and hole electron density were 3.11 and -2.36 e A^{-3}. The least-squares refinement converged normally with residuals of $R_1 = 0.0538$ and GOF = 0.996. Crystal and refinement data for **9**: formula $C_{86}H_{108}N_8O_4Si_4Fe_2U_2$ $4(C_6H_6)$, space group $P\bar{1}$, $a = 10.818(4)$,

$b = 15.243(5)$, $c = 16.736(5)$, $\alpha = 70.951(3)$, $\beta = 81.575(4)$, $\gamma = 89.130$ $(4)°$, V = 2578.9(15) Å^3, Z = 1, $\mu = 3.507$ mm^{-1}, $F(000) = 1172$, $R_1 = 0.0815$ and $wR_2 = 0.1240$ (based on all 12176 data, $I > 2\sigma(I)$).

Appendix A. Supporting information

Experimental details for compound characterization and full crystallographic descriptions (as cif) are available as supplementary material at doi:10.1016/j.jorganchem.2010.08.003.

References

[1] S.D. Gray, K.J. Weller, M.A. Bruck, P.M. Briggs, D.E. Wigley, J. Am. Chem. Soc. 117 (1995) 10678–10693.
[2] S.D. Gray, D.P. Smith, M.A. Bruck, D.E. Wigley, J. Am. Chem. Soc. 114 (1992) 5462–5463.
[3] K.J. Weller, S.D. Gray, P.M. Briggs, D.E. Wigley, Organometallics 14 (1995) 5588–5597.
[4] K.J. Weller, P.A. Fox, S.D. Gray, D.E. Wigley, Polyhedron 16 (1997) 3139–3163 and references therein.
[5] K.J. Weller, I. Filippov, P.M. Briggs, D.E. Wigley, Organometallics 17 (1998) 322–329.
[6] K.J. Weller, I. Filippov, P.M. Briggs, D.E. Wigley, J. Organomet. Chem. 528 (1997) 225–228.
[7] K.D. Allen, M.A. Bruck, S.D. Gray, R.P. Kingsborough, D.P. Smith, K.J. Weller, D.E. Wigley, Polyhedron 14 (1995) 3315–3333.
[8] T.S. Kleckley, J.L. Bennett, P.T. Wolczanski, E.B. Lobkovsky, J. Am. Chem. Soc. 119 (1997) 247–248.
[9] J.B. Bonanno, A.S. Veige, P.T. Wolczanski, E.B. Lobkovsky, Inorg. Chim. Acta 345 (2003) 173–184.
[10] K.J. Covert, D.R. Neithamer, M.C. Zonnevylle, R.E. LaPointe, C.P. Schaller, P.T. Wolczanski, Inorg. Chem. 30 (1991) 2494–2508.
[11] D.R. Neithamer, L. Parkanyi, J.F. Mitchell, P.T. Wolczanski, J. Am. Chem. Soc. 110 (1988) 4421–4423.
[12] A.R. Fout, B.C. Bailey, J. Tomaszewski, D.J. Mindiola, J. Am. Chem. Soc. 129 (2007) 12640–12641.
[13] B.C. Bailey, H. Fan, J.C. Huffman, M.H. Baik, D.J. Mindiola, J. Am. Chem. Soc. 128 (2006) 6798–6799.
[14] P.L. Diaconescu, Curr. Org. Chem. 12 (2008) 1388–1405.
[15] M.A. Huertos, J. Perez, L. Riera, J. Am. Chem. Soc. 130 (2008) 5662–5663.
[16] M.A. Huertos, J. Pérez, L. Riera, A. Menéndez-Velázquez, J. Am. Chem. Soc. 130 (2008) 13530–13531.
[17] A. Sattler, G. Parkin, Nature 463 (2010) 523–526.
[18] J.A. Pool, B.L. Scott, J.L. Kiplinger, Chem. Commun. (2005) 2591–2593.
[19] A. Arunachalampillai, P. Crewdson, I. Korobkov, S. Gambarotta, Organometallics 25 (2006) 3856–3866.
[20] A.W. Wong, K.L. Miller, P.L. Diaconescu, Dalton Trans. 39 (2010) 6726–6731.
[21] C.T. Carver, M.J. Monreal, P.L. Diaconescu, Organometallics 27 (2008) 363–370.
[22] C.T. Carver, D. Benitez, K.L. Miller, B.N. Williams, E. Tkatchouk, W.A. Goddard, P.L. Diaconescu, J. Am. Chem. Soc. 131 (2009) 10269–10278.
[23] K.L. Miller, B.N. Williams, D. Benitez, C.T. Carver, K.R. Ogilby, E. Tkatchouk, W.A. Goddard, P.L. Diaconescu, J. Am. Chem. Soc. 132 (2010) 342–355.
[24] S. Jie, P.L. Diaconescu, Organometallics 29 (2010) 1222–1230.
[25] S. Duhović, S. Khan, P.L. Diaconescu, Chem. Commun. 46 (2010) 3390–3392.
[26] M.J. Monreal, P.L. Diaconescu, Organometallics 27 (2008) 1702–1706.
[27] A. Shafir, M.P. Power, G.D. Whitener, J. Arnold, Organometallics 19 (2000) 3978–3982.
[28] A. Shafir, J. Arnold, J. Am. Chem. Soc. 123 (2001) 9212–9213.
[29] M.J. Monreal, C.T. Carver, P.L. Diaconescu, Inorg. Chem. 46 (2007) 7226–7228.
[30] S. Duhović, M.J. Monreal, P.L. Diaconescu, Inorg. Chem. 49 (2010) 7165–7169.
[31] M.J. Monreal, S. Khan, P.L. Diaconescu, Angew. Chem. Int. Ed. 48 (2009) 8352–8355.
[32] C.T. Carver, P.L. Diaconescu, J. Alloys Compd. 488 (2009) 518–523.
[33] C.T. Carver, P.L. Diaconescu, J. Am. Chem. Soc. 130 (2008) 7558–7559.
[34] C.T. Carver, B.N. Williams, K.R. Ogilby, P.L. Diaconescu, Organometallics 29 (2010) 835–846.
[35] P.L. Diaconescu, Acc. Chem. Res. (2010). doi:10.1021/ar1000605.
[36] M.J. Monreal, P.L. Diaconescu, J. Am. Chem. Soc. 132 (2010) 7676–7683.
[37] S.E. Whitney, B. Rickborn, J. Org. Chem. 56 (1991) 3058–3063.
[38] M.C. Pirrung, S. Ghorai, T.R. Ibarra-Rivera, J. Org. Chem. 74 (2009) 4110–4117.
[39] A.B. Pangborn, M.A. Giardello, R.H. Grubbs, R.K. Rosen, F.J. Timmers, Organometallics 15 (1996) 1518–1520.